Surface alignment of liquid crystal multilayers evaporated on photoaligned polyimide film observed by surface profiler

ELSEVIER

Science and Technology of Advanced Materials 6 (2005) 149–157

SCIENCE AND TECHNOLOGY OF ADVANCED MATERIALS

www.elsevier.com/locate/stam

Surface alignment of liquid crystal multilayers evaporated on photoaligned polyimide film observed by surface profiler

Thet Naing Oo[a,*], Tetsuya Iwata[b], Munehiro Kimura[a], Tadashi Akahane[a]

[a]*Department of Electrical Engineering, Faculty of Engineering, Nagaoka University of Technology, 1603-1 Kamitomioka, Nagaoka, Niigata 940-2188, Japan*
[b]*Core System Co., Ltd, 2-2-2 Nakajima, Nagaoka, Niigata 940-0094, Japan*

Received 26 August 2004; revised 4 October 2004; accepted 10 November 2004

Abstract

The investigation of the surface alignment of liquid crystal (LC) multilayers evaporated on photoaligned polyimide vertical alignment (PI-VA) film was carried out by means of the novel three-dimensional (3D) surface profiler. We report the first use of the surface profiler to visualize a microscopic image of the monolayer arrangement of LC molecules in contact with the surface of photo-treated PI-VA film. The photoinduced anisotropy of partially UV-exposed PI-VA film can be visualized as a topological image of LC multilayers. It seems that the topology of LC multilayers is indicating the orientational distribution of LC molecules on the treated film. It was found that the periodically photoaligned PI-VA film surface can align an adsorbed LC monolayer and the LC molecular alignment can be extended to the bulk via the epitaxylike LC–LC interaction, i.e. a short-range molecular interaction. With regard to the unexposed PI-VA film surface, noticeable anisotropy in the monolayer alignment was not observed, indicating that the long-range elastic interaction may be responsible for the bulk alignment. The appearance of small droplets in the masked region may be presumably related to the dewetting phenomena.

Keywords: Surface alignment; Photoalignment; Liquid crystal; Polyimide film; Surface profiler; Dewetting

1. Introduction

Liquid crystals (LCs) can be easily oriented by contact with surfaces on a macroscopic scale [1]. The phenomenon of orientation of LCs by surfaces is a topic of crucial significance for applications of these materials, especially for liquid crystal displays (LCDs) [2]. To fabricate a commercial product of LCD, uniform orientation of the LC molecules is required. The alignment of a LC by the surface treatment of a substrate has been one of the essential aspects of LC behavior. It is usually achieved by using polymer alignment films deposited on glass substrates. Hence, alignment films are key components in LCDs. Homogeneous alignment occurs when the LC director aligns parallel to the substrate, whereas perpendicular alignment is referred to as homeotropic. To achieve a homogeneous alignment, a preferred orientation to the alignment by physically or chemically treating the surface must be provided. Rubbing the surface has been a simple way of achieving a preferred orientation. However, rubbing may produce dust, static charging and mechanical damage which deteriorates the production yield. One of the more attractive alternatives to rubbing is the generation of a surface anisotropy of an alignment film by photochemical reaction called "photo-photoinduced alignment" [3]. In general, photoinduced alignment is achieved by exposing with both unpolarized and polarized ultraviolet (UV) light on a photoalignment polymer film. There are three main kinds of materials that are used for photoalignment layers. They can be categorized according to the photochemical reaction responsible for the photoalignment, viz. (i) azo-containing polymers (photoalignment by reversible *cis–trans* isomerization), (ii) crosslinkable materials (photoalignment by photo-dimerization), and (iii) polyimides (photoalignment by photodegradation) [4].

* Corresponding author. Tel.: +81 258 466000 5321; fax: +81 258 479500.
E-mail address: tno2002@nagaokaut.ac.jp (T. Naing Oo).

1468-6996/$ - see front matter © 2005 Elsevier Ltd. All rights reserved.
doi:10.1016/j.stam.2004.11.009

The understanding of surface effects and anchoring in LCs requires profound knowledge of the LC–surface interaction. The nature of the LC–surface interaction is complex and the most important factors include van der Waals interactions, dipolar interactions, steric interactions, hydrogen and chemical bonding, and surface topography [5]. Despite the enormous theoretical and practical relevance of surface anchoring, the underlying mechanisms are not very well understood [2]. In particular, there are two models of alignment mechanisms to elucidate surface-induced bulk alignment in the case of nematic LCs, viz. (i) Berreman's groove model and (ii) molecular epitaxylike model [6,7]. The first model is anisotropic LC orientational elasticity in connection with rubbing-induced microgrooves [8–10]. The second model is short-range interactions on the molecular scale [7,11–15]. In regard to the first model, Berreman proposed that the director field adapts itself to the geometrical topology of the substrate surface to minimize the elastic strain energy arising from the distortions of the director field. The second model is based on interactions between the LC molecules and the substrate. These interactions affect the orientational order of the LC molecules in the vicinity of the substrate; resultant LC molecular order in turn propagates toward the bulk via the intermolecular interactions which tend to align the molecules parallel to each other. The aligning action evolves from the substrate to the bulk LC via a specific interfacial region [2,16,17]. This means that the bulk molecules exhibit epitaxial growth of nematic phase from the alignment surface [7,18]. The anisotropic surface–LC interaction by which the surface governs the orientation of the bulk is often termed surface orientational anchoring [2].

For a better understanding of the surface effect on the alignment of LCs, many studies are paying special attention to the interfacial properties of LCs. To clearly characterize the microscopic features of surfaces and interfaces, many types of imaging techniques have been developed over the years such as second harmonic generation (SHG) measurements, scanning tunneling microscopy (STM) and atomic force microscopy (AFM). However, each technique has some limitations and practical difficulties. In SHG technique, the signal increases with decreasing spot size for a given laser power but may be eventually limited by laser-induced surface damage. The problems involved in SHG technique are considerations about the size of the area to be probed, and the surface damage threshold of the material caused by laser heating [19]. Moreover, inside of the probed area should be uniform in regard to SHG technique because inhomogeneous surface area can generate the variations in SHG signal [20]. For STM technique, one of the practical difficulties is that it requires a conducting substrate. Moreover, flatness is a major requirement for a good STM substrate [21,22]. A number of STM experiments revealed images of LC molecules physisorbed on atomically flat and chemically inert crystals (graphite, molybdenum disulphide, etc…). However, STM images of LC molecules on the rubbed polyimide (PI) surface have not yet been achieved [23]. Besides, Fang et al. reported the tip-induced effect on the arrangement of liquid crystal molecules. This effect was such that the STM tip immersed in the drop of the liquid crystal molecules may change their arrangement by the influence of the electrical field [24]. Thus, the imaging mechanism and the physical interpretation of the STM images of these organic systems remain to be resolved. In regard to AFM technique, it does not require electrically conductive surfaces [21]. AFM can produce images of topography of conducting and nonconducting materials by scanning a sharp tip mounted on a cantilever-type spring over a sample surface. Typical resolution of AFM is on the nanometer and angstrom scale. However, the interpretation of atomic resolution AFM images depends critically on the details of the tip–sample interaction [25]. AFM can reveal an image of a rubbed PI film surface, but the resolution is often not sufficient to resolve a single polymer chain [26]. Most of the topographic images of surfaces with adsorbed organic molecules collected with the AFM have been recorded in the contact mode. In this contact mode, there is a destructive influence of the lateral forces, due to the relative movement of the tip with respect to the sample. One way to overcome this problem is to operate the AFM with the sample, tip and cantilever immersed in a liquid such as oil or water [25,27]. Therefore, to overcome some of these limitations and practical difficulties encountered by contemporary imaging techniques and to visualize a microscopic image of the monolayer arrangement of LC molecules in contact with the surface of photo-treated PI-VA film, we have carried out this investigation by means of novel surface profiler instrument. As will be discussed later, the fundamental concept of this surface profiler is based on the detection of angular deflection of a fast-scanning laser beam in a noncontact manner [28]. In contrast to STM, it does not require a conducting and flat substrate. Laser-induced surface damage effect encountered in SHG technique can be overcome because the scan speed of the laser beam spot on substrate surface is 5 mm/ms. Since it is a form of noncontact technique which maps surface topography, there is no need to consider tip-induced effect and tip-sample interaction found in STM and AFM. It can be used to produce noncontact images with high vertical resolution ($\sim$0.01 nm) and our research shows that this technique turns out to be a useful technique in its own ways.

In our previous study, we used polyvinylcinnamate as a photoalignment layer [29]. In this work, we used PI-VA as a photoalignment layer that originally exhibited homeotropic alignment. The optical anisotropy of the PI-VA is due to the photodegradation effect under the irradiation of polarized or unpolarized UV light. To elucidate a basic concept of photodegradation effect, we would like to revisit original works of literature. Hasegawa and Taira [30] first reported that a PI film exposed to linearly polarized ultraviolet (LPUV) light induces a uniform

parallel (homogeneous) alignment of LC molecules. The average molecular orientation of the LC molecules is parallel to the film surface and perpendicular to the polarization direction of the LPUV light. They explained this LC alignment from the viewpoint of anisotropic photodepolymerization of the PI main chains. The PI chain oriented parallel to the polarization direction of the irradiated LPUV light is broken more easily than that oriented perpendicular to it. Thus, the orientational distribution of the PI chains becomes anisotropic after LPUV exposure. This anisotropic orientation of the PI chains aligns the LC molecules perpendicular to the polarization direction which corresponds to the direction of the maximum density of undegraded polyimide chains on exposure. Yoshida et al. [31], Li et al. [32], and Iimura et al. [33] also realized that the tilted homeotropic alignment was achieved by irradiation of unpolarized and polarized UV light on a PI film that originally exhibited homeotropic alignment. In these studies, they confirmed that the optical anisotropy of the PI resulted from the photodepolymerization of the alkyl branch in the film. Yoshida et al. [31], and Iimura et al. [33] also demonstrated that the p-component of the incident UV light contributes to the pretilt angle generation but the s-component cannot give a tilted polymer distribution due to the circular symmetry in the plane of incidence.

The purpose of this investigation is to study the surface alignment of LC multilayers evaporated on photoinduced PI-VA film and to visualize a microscopic image of the monolayer arrangement of LC molecules in contact with the surface of PI-VA film. We aim to investigate the alignment of LC molecules on a periodically patterned substrate surface to see a clear picture of different alignment mechanism. In this paper, the surface alignment of LC multilayers evaporated on photoinduced PI-VA film was investigated by means of the 3D surface profiler and the optical polarizing microscope.

2. Concept of the 3D surface profiler

The alignment process of adsorbed LC monolayers on the surface of photoinduced PI-VA alignment film can be imagined as a microscopic image. The surface topology of the LC multilayers was investigated by means of Scanning Laser Imaging Scope (Core System Co., Ltd), which was the novel instrument for 3D surface profile. Fig. 1(a) depicts the fundamental concept of the profile measurement. Suppose a curved object with maintaining the distance l from the light source to the surface S. Scanning direction is along the x-axis. The surface profile of the measured object along the x-axis can be expressed by the function $f(x)$. Let us assume that the light beam from the laser light source L is emitted on the curved object at the point **P**. When the angle θ with respect to the x-axis is much less than 1, the gradient at **P** can be

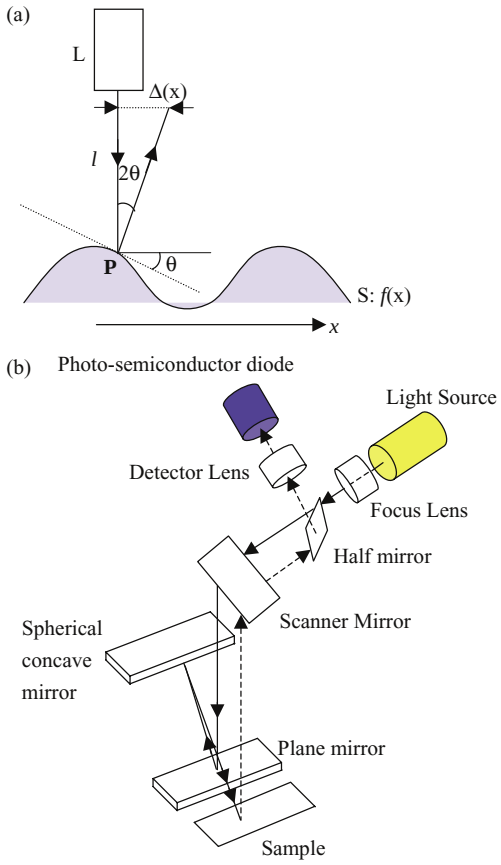

Fig. 1. (a) Basic concept of the profile measurement; (b) Schematic diagram of 3D surface profiler.

expressed by:

$$\frac{df(x)}{dx} = \tan\theta \sim \theta \tag{1}$$

The angle between the incident light and the reflected light is approximated to 2θ, which corresponds to the deviation Δ from the incident light beam. Under such condition, Δ is approximated to $2\theta l$. When the deviation Δ is measured by scanning object, the distribution function of the surface profile f(x) can be obtained by the measurement of Δ(x).

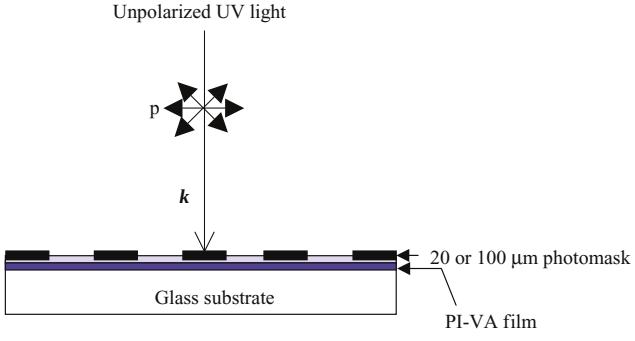

Fig. 2. Method of exposure to unpolarized UV light. Here p stands for the randomly oriented polarization directions of the incident unpolarized UV light and **k** denotes the propagation vector.

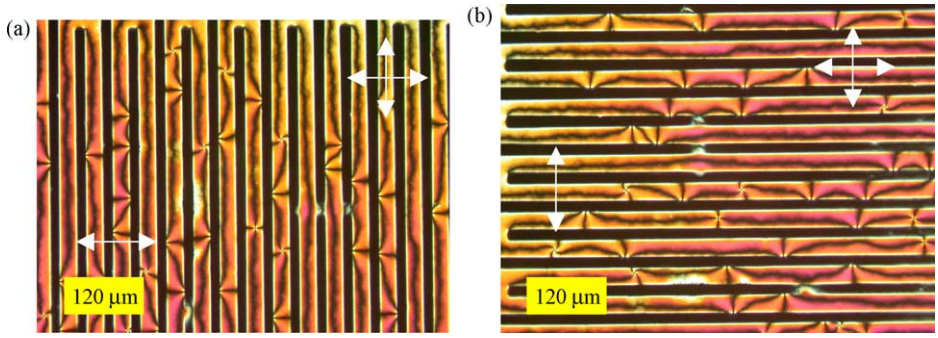

Fig. 3. Polarized microphotographs of the photoaligned LC cell between crossed polarizers.

From the equation (1), $f(x)$ can be derived by:

$$\alpha \int dx \Delta(x) = \int dx \theta(x) = f(x) \quad (2)$$

where $\alpha = 1/2\ l$. The coefficient α can be determined by the calibration measurement with the known object. Sequential scanning with the 2D direction can provide the 3D surface profile.

The contrivance for surface profiler is illustrated in Fig. 1(b). In this surface profiler, scanner mirror plays the role instead of scanning detector. This surface profiler was devised as such that the spherical concave mirror was combined for the purpose of synchronizing the curvature with optical intensity at the measured point.

3. Experimental procedure

Corning-1737F (Corning Co.) glass was used as a substrate. As a photoalignment layer, we used PI-VA film [1 wt%, Nissan Chemical] that originally exhibited homeotropic alignment. This material was spin-coated on the glass substrates and then baked at 200 °C for 1 h. The chemical formulation of this polyimide is not available because of commercial confidentiality.

The PI-VA film was exposed with unpolarized UV light ($\lambda = 320$ nm) using UV light guide (Suncure 202, Asahi Glass Company) at normal incidence (Fig. 2). The periodical striped patterns were produced by means of a photomask (20 μm for fabrication of a cell and 100 μm for surface profiler measurement). The intensities of the UV light after passing through the 20 μm and 100 μm photomasks are 60 and 70 mW/cm^2, respectively. The exposure time was set to be 30 min. To verify the flatness of PI-VA film, atomic force microscope (AFM) (Shimadzu, SPM-9500J2) was used. Exposure patterns for alignment will be alternating exposed (random planar) and unexposed (homeotropic) stripes. To examine these alignment patterns, LC cells with a cell gap of 5 μm were made using one exposed substrate and the other unexposed. The cells were filled with 4′-*n*-pentyl-4-cyanobiphenyl (5CB, supplied by Merck) by capillary action in the isotropic phase and cooled to room temperature. The LC alignment of the cell was checked by optical polarizing microscope (OPM). For evaporation, 4′-*n*-pentyl-4-cyanobiphenyl (5CB, supplied by Merck) [$T_{NI} = 35.5$ °C] was heated on a hot plate at 90 °C and was adsorbed on the substrate surface positioned 50 mm from the LC source at room temperature in air. 5CB adsorption was controlled by the duration of evaporation. The alignment process of adsorbed LC monolayers on the surface of photoinduced PI-VA alignment film can be imagined as a microscopic image. The surface topology of the LC multilayers was investigated by means of the novel 3D surface profiler

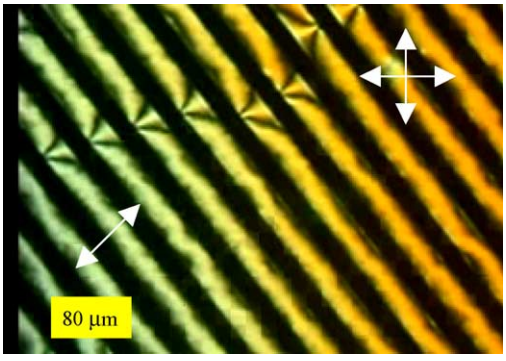

Fig. 4. Polarized microphotograph of the photoaligned LC cell for the polarizer and analyzer at 45°.

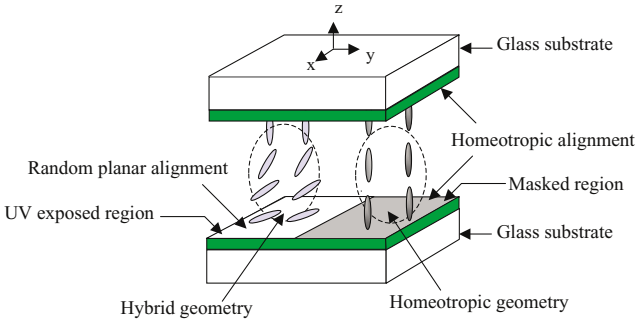

Fig. 5. The photoaligned LC cell having alternating exposed and unexposed striped patterns.

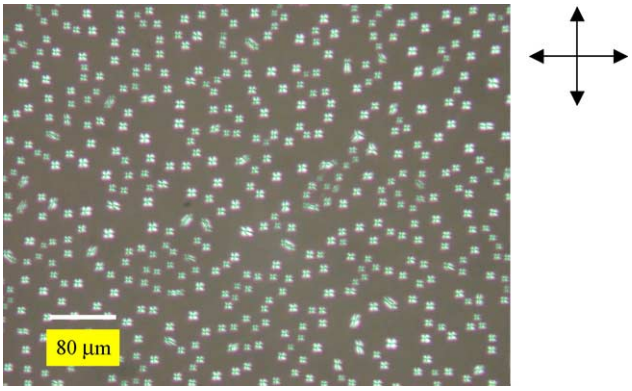

Fig. 6. Polarized microphotograph of the evaporated surface of unexposed PI-VA film for 3 h evaporation under crossed polarizers.

instrument (Scanning Laser Imaging Scope, Core System Co., Ltd). The remarkable features of this instrument are its wide range of scanning area (~40 mm) and high vertical resolution (~0.01 nm). Notice that the negative sign has no physical meaning for the vertical measurement scale of the surface profiler in nanometer.

4. Results and discussion

4.1. LC alignment behavior of photoinduced PI-VA film

Fig. 3 shows polarized microphotographs of a photo-aligned LC cell between crossed polarizers. The alternating exposed and unexposed striped patterns can be clearly seen. The exposed region produces a random planar alignment with nematic schlieren texture. In the middle of each exposed region, there is a uniform planar line because this black line became bright, yielding hybrid orientation for the polarizer and analyzer at 45° (Fig. 4). In the unexposed region, the LC alignment is homeotropic since extinction is observed between the crossed polarizers. These alignment patterns can be imagined with the aid of Fig. 5. The results are in good agreement with the previous elucidation of photodegradation effect.

4.2. Surface alignment of LC molecules evaporated on unexposed PI-VA film

Fig. 6 shows a polarized microphotograph of the evaporated surface of unexposed PI-VA film for 3 h evaporation. Under crossed polarizers, very tiny homeotropic droplets (of the order of µm) were found due to the dewetting phenomena. This occurs when the surface energy of the PI-VA film is less than the sum of the interfacial energy between PI-VA and LC films and the surface energy of LC film. Fig. 7 shows 3D surface height pattern mapping of the LC evaporated surface of unexposed PI-VA film for 3 h evaporation. From this pattern mapping, it was also found that the height of the surface topological roughness seems to be less than 0.1 nm. These results suggest that LC molecules were not adsorbed on unexposed PI-VA film surface for sufficient time span of 3 h evaporation and the surface density of LC molecules is quite low, i.e. the growth of the first adsorbed LC monolayer cannot take place during this 3 h

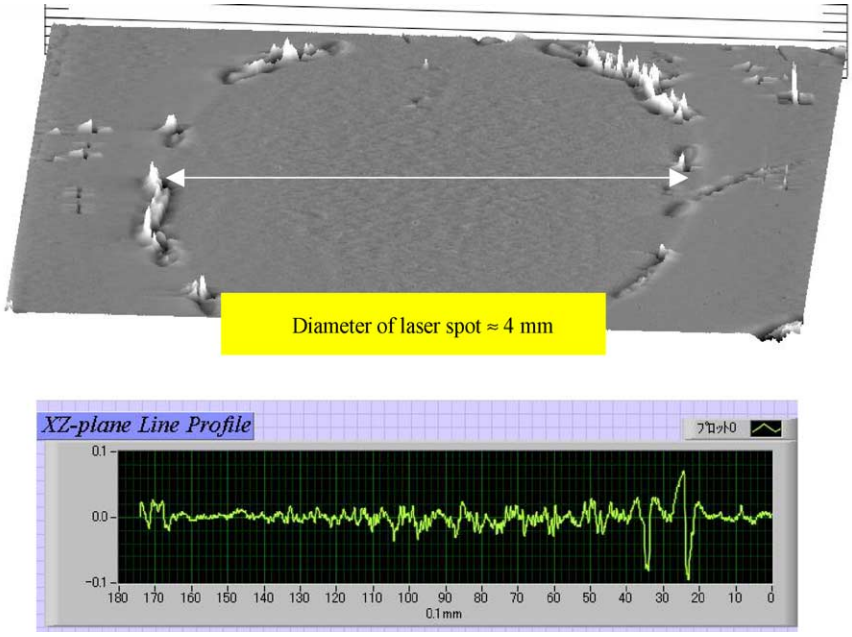

Fig. 7. 3D surface height pattern mapping of the evaporated surface of unexposed PI-VA film for 3 h evaporation.

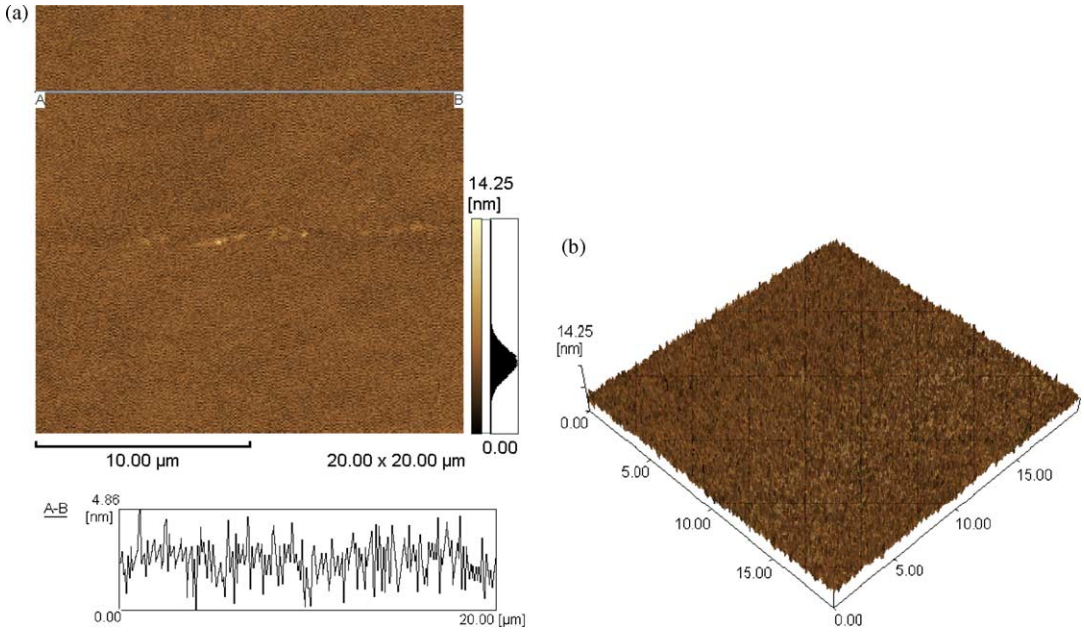

Fig. 8. 20×20 μm^2 dynamic mode AFM images of the surface of photoinduced PI-VA alignment film. (a) 2D display of the AFM data; (b) 3D display of the AFM data.

time span, resulting in the formation of very small droplets probably due to dewetting phenomena [34–36].

4.3. Surface alignment of LC multilayers evaporated on photoinduced PI-VA film

To verify the flatness of PI-VA film, dynamic mode AFM images of photoinduced PI-VA film were taken. We used 20 μm photo-mask instead of 100 μm photo-mask because the scanning range of our AFM is 30×30 μm^2. Fig. 8 shows that the surface of photoinduced PI-VA alignment film did not reveal periodical surface relief gratings but had a surface topology with a few angstrom surface roughness.

Figs. 9 and 10 show 3D surface height pattern mappings of the evaporated surface of unpolarized

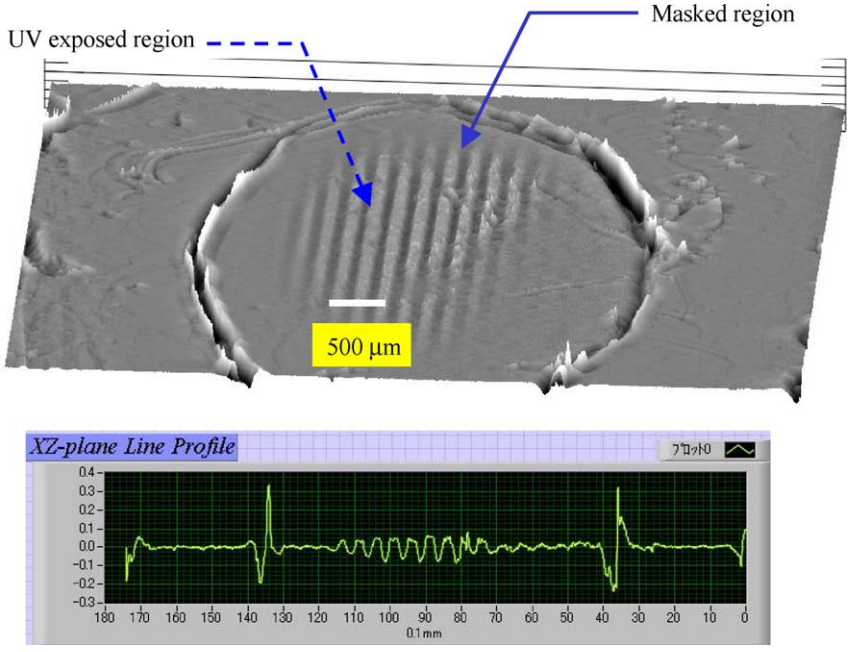

Fig. 9. 3D surface alignment pattern mapping of the evaporated surface of unpolarized UV-exposed PI-VA alignment film taken by the surface profiler for 2 h evaporation. Vertical height information: ≈0.16 nm (max.) for UV exposed region and a few angstrom surface roughness for the masked region.

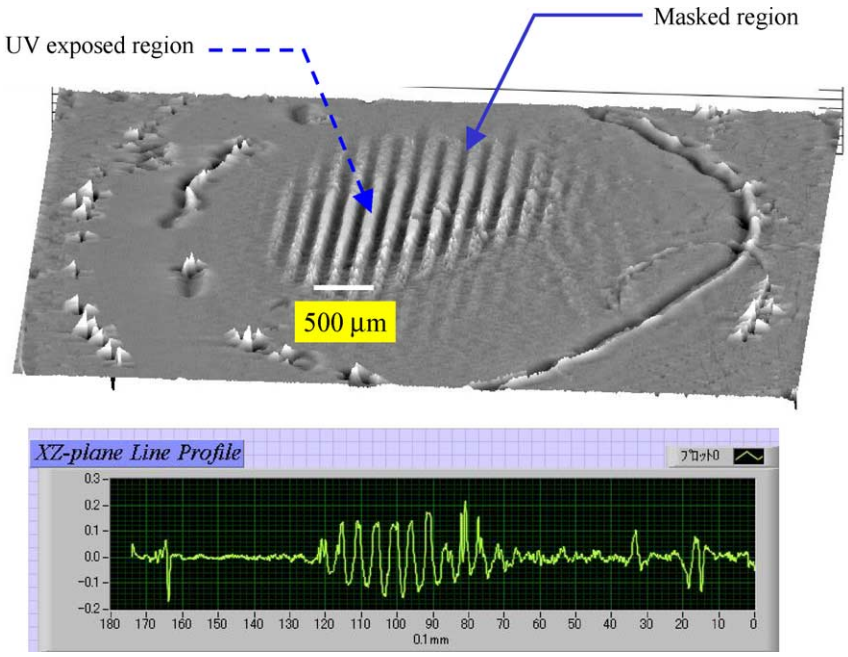

Fig. 10. 3D surface alignment pattern mapping of the evaporated surface of unpolarized UV-exposed PI-VA alignment film taken by the surface profiler for 3 h evaporation. Vertical height information: ≈0.28 nm (max.) for UV exposed region and a few angstrom surface roughness for the masked region.

UV-exposed (with 100 µm photomask) PI-VA film for 2 and 3 h evaporation, respectively. At both 2 and 3 h 5CB evaporation, a periodic profile can be clearly seen, where the period corresponds to the photomask pattern (100 µm line and space). Based on the result of Fig. 7, it was recognized that the height of UV exposed region is greater than that of the masked region. This result implies that the surface molecular alignment at the UV exposed region is voluminous compared with the masked region. On the other hand, it is known from the measurement of LC cell alignment (Fig. 3) that the surface LC molecules are randomly oriented in the UV exposed region due to the selective photodecomposition of the alkyl branches when the PI-VA film is exposed to unpolarized UV light. In order to validate these results, Fig. 11(a) and (b) show polarized microphotographs of the evaporated surface of unpolarized UV-exposed PI-VA film for 2 and 3 h evaporation, respectively. Fig. 12 is the magnification of Fig. 11(b). Periodic images can also be clearly seen in Figs. 11 and 12. In the UV exposed region, a random planar alignment was found whereas homeotropic droplets appeared in the masked region.

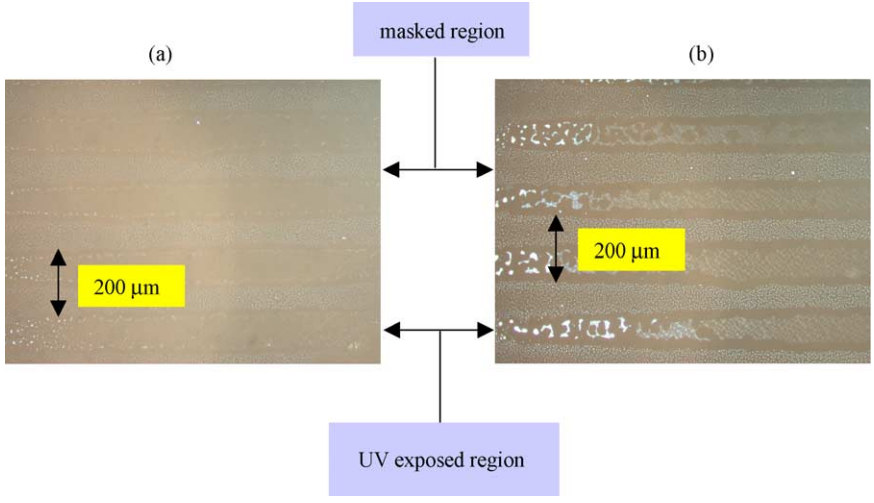

Fig. 11. Polarized microphotographs of the evaporated surface of unpolarized UV-exposed PI-VA alignment film for (a) 2 h (b) 3 h evaporation, under crossed polarizers.

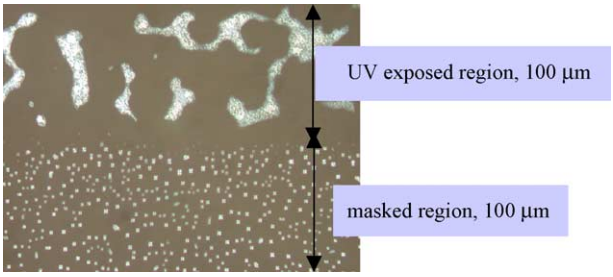

Fig. 12. Magnification of Fig. 11(b) under crossed polarizers.

5. Conclusions

The following experimental findings were made by the novel surface profiler instrument and the optical polarizing microscope.

(1) The random planar alignment was realized by irradiation of normally incident unpolarized UV light on photoalignment PI-VA film that originally exhibited homeotropic alignment.
(2) The surface alignment of LC multilayers evaporated on photoaligned PI-VA film exhibited a periodic profile.
(3) The height of LC multilayers in the UV exposed region was greater than that in the masked region. This height difference revealed the different alignment mechanisms for the exhibited periodic profile.
(4) By means of the optical polarizing microscopy, the random planar alignment in the UV exposed region and homeotropic droplets in the masked region were found and observed.
(5) The photoinduced PI-VA film surface can align an adsorbed LC monolayer and then the alignment can be extended to the bulk via the epitaxylike LC–LC interaction i.e. a short-range molecular intertaction.
(6) For the unexposed PI-VA film surface, noticeable anisotropy in the monolayer alignment was not observed, indicating that the long-range elastic interaction may be responsible for the bulk alignment.
(7) The appearance of very small droplets in the masked region may be presumably related to dewetting phenomena.

The surface alignment of LC multilayers evaporated on practically used polyimide film has been demonstrated by means of the novel surface profiler, opening a new area of research in surface alignment of LCs. Furthermore, it is shown that the open-air LC deposition on the patterned alignment is a potential technique to realize a functional surface.

Acknowledgements

This work was partially supported by a Grant-in-Aid for Encouragement of Young Scientists (B) (No. 15760020) from Japan Society for the Promotion of Science and 21st century COE program "Creation of Hybridized Materials with Super-Functions and Formation of International Research and Education Centre" from Ministry of Education, Culture, Sports, Science and Technology, Japan.

References

[1] A.A. Sonin, The Surface Physics of Liquid Crystals, Gordon and Breach, Amsterdam, 1995.
[2] B. Jérôme, Surface effects and anchoring in liquid crystals, Rep. Prog. Phys. 54 (1991) 391–451.
[3] W.M. Gibbons, P.J. Shannon, S.T. Sun, B.J. Swetlin, Surface-mediated alignment of nematic liquid crystals with polarized laser light, Nature 351 (1991) 49–50.
[4] M. O'Neill, S.M. Kelly, Photoinduced surface alignment for liquid crystal displays, J. Phys. D: Appl. Phys. 33 (2000) R67–R84.
[5] K. Okano, N. Matsuura, S. Kobayashi, Alignment of a liquid crystal on an anisotropic substrate, Jpn J. Appl. Phys. 21 (1982) L109–L110.
[6] W. Chen, M.B. Feller, Y.R. Shen, Investigation of anisotropic molecular orientational distributions of liquid-crystal monolayers by optical second-harmonic generation, Phys. Rev. Lett. 63 (1989) 2665–2668.
[7] M.B. Feller, W. Chen, Y.R. Shen, Investigation of surface-induced alignment of liquid-crystal molecules by optical second-harmonic generation, Phys. Rev. A 43 (1991) 6778–6792.
[8] D.W. Berreman, Solid surface shape and the alignment of an adjacent nematic liquid crystal, Phys. Rev. Lett. 28 (1972) 1683–1686.
[9] D.W. Berreman, Alignment of liquid crystal by grooved surfaces, Mol. Cryst. Liq. Cryst. 23 (1973) 215–231.
[10] S. Faetti, Azimuthal anchoring energy of a nematic liquid crystal at a grooved interface, Phys. Rev. A 36 (1987) 408–410.
[11] J.M. Geary, J.W. Goodby, A.R. Kmetz, J.S. Patel, The mechanism of polymer alignment of liquid-crystal materials, J. Appl. Phys. 62 (1987) 4100–4108.
[12] D. Johannsmann, H. Zhou, P. Sonderkaer, H. Wierenga, B.O. Myrvold, Y.R. Shen, Correlation between surface and bulk orientations of liquid crystals on rubbed polymer surfaces: odd–even effects of polymer spacer units, Phys. Rev. E 48 (1993) 1889–1896.
[13] H. Kikuchi, J.A. Logan, D.Y. Yoon, Study of local stress, morphology, and liquid-crystal alignment on buffed polyimide surfaces, J. Appl. Phys. 79 (1996) 6811–6817.
[14] J. Cheng, G.D. Boyd, The liquid-crystal alignment properties of photolithographic gratings, Appl. Phys. Lett. 35 (1979) 444–446.
[15] R. Barberi, I. Dozov, M. Giocondo, M. Iovane, Ph. Martinot-Lagarde, D. Stoenescu, S. Tonchev, L.V. Tsonev, Azimuthal anchoring of nematic on undulated substrate: Elasticity versus memory, Eur. Phys. J. B 6 (1998) 83–91.
[16] J. Cognard, Alignment of nematic liquid crystals and their mixtures, Mol. Cryst. Liq. Cryst. (Suppl. Ser.) A5 (1982) 1–74.
[17] B. Jérôme, Surface alignment, in: D. Demus, J. Goodby, G.W. Gray, H.-W. Spiess, V. Vill (Eds.), Handbook of Liquid Crystals, vol. 1, (1998), pp. 535–548.
[18] M. Barmentlo, R.W.J. Hollering, N.A.J.M. van Aerle, Correlations between surface and bulk liquid-crystal alignment observed with optical second-harmonic generation, Phys. Rev. A 46 (1992) R4490–R4493.
[19] G.T. Boyd, Y.R. Shen, T.W. Hänsch, Continuous-wave second-harmonic generation as a surface microprobe, Opt. Lett. 11 (1986) 97–99.
[20] K. Pedersen, S.I. Bozhevolnyi, Second-harmonic generation scanning microscopy on domains in Al surfaces, Phys. Stat. Sol. (a) 175 (1999) 201–206.

[21] J. Frommer, Scanning tunneling microscopy and atomic force microscopy in organic chemistry, Angew. Chem. Int. Ed. Engl. 31 (1992) 1298–1328.
[22] P.K. Hansma, J. Tersoff, Scanning tunneling microscopy, J. Appl. Phys. 61 (1987) R1–R23.
[23] M.R. Hernandez, M.J. Miles, Scanning tunneling microscopy studies of phase transitions in liquid crystals, Scanning Microscopy 12 (1998) 235–241.
[24] J.Y. Fang, Z.H. Lu, G.W. Ming, Z.M. Ai, Y. Wei, P. Stroeve, Anchoring structure of liquid-crystal monolayers on polyimide Langmuir–Blodgett films observed by scanning tunneling microscopy, Phys. Rev. A 46 (1992) 4963–4965.
[25] D. Rugar, P. Hansma, Atomic force microscopy, Phys. Today Oct. 43 (1990) 23–30.
[26] Y.M. Zhu, L. Wang, Z.H. Lu, Y. Wei, X.X. Chen, J.H. Tang, Atomic force microscopic study of rubbed polyimide films, Appl. Phys. Lett. 65 (1994) 49–51.
[27] O. Marti, B. Drake, P.K. Hansma, Atomic force microscopy of liquid-covered surfaces: Atomic resolution images, Appl. Phys. Lett. 51 (1987) 484–486.
[28] R. Shinozaki, O. Sasaki, T. Suzuki, Fast scanning method for one-dimensional surface profile measurement by detecting angular deflection of a laser beam, Appl. Opt. 43 (2004) 4157–4163.
[29] T.N. Oo, Y. Ohta, N. Tanaka, T. Iwata, M. Kimura, T. Akahane, Study of surface alignment of liquid crystal multilayers evaporated on polyvinylcinnamate photoalignment film, Adv. Tech. Mat. Mat. Proc. J. (ATM), in press.
[30] M. Hasegawa, Y. Taira, Nematic homogeneous photoalignment by polyimide exposure to linearly polarized UV, J. Photopolym. Sci. Technol. 8 (1995) 241–248.
[31] H. Yoshida, Y. Koike, Inclined homeotropic alignment by irradiation of unpolarized UV light, Jpn J. Appl. Phys. 36 (1997) L428–L431.
[32] H.F. Li, E.J. Kim, H. Furue, Y. Iimura, S. Kobayashi, Control of pretilt angle and its direction in homeotropic alignment of liquid crystals using photoalignment technique, Mol. Cryst. Liq. Cryst. 326 (1999) 249–257.
[33] Y. Iimura, S. Kobayashi, Prospects of the photo-alignment technique for LCD fabrication, SID 97 (1997) 311–314.
[34] M. Woolley, R.H. Tredgold, P. Hodge, Ultrathin films of smectic liquid crystals on solid substrates, Langmuir 11 (1995) 683–686.
[35] M. Bardosova, R.H. Tredgold, Ultra-thin films of smectic liquid crystals on solid substrates, Mol. Cryst. Liq. Cryst. 355 (2001) 289–303.
[36] I. Drevenšek Olenik, K. Kočevar, I. Muševič, Th. Rasing, Structure and polarity of 8CB films evaporated onto solid substrates, Eur. Phys. J. E 11 (2003) 169–175.